Hydrogen Gas Sensor of ZnO Doping with CuO/PS Nanocomposite

The 5th International scientific Conference on Nanotechnology& Advanced Materials Their Applications (ICNAMA 2015)3-4 Nov, 2015

Dr .Isam M. Ibrahim
Collage of science, University of Baghdad/ Baghdad.
Email: Shahad.e.sharhan@gmail.com
Shahad I.sharhan
Collage of science, University of Baghdad/ Baghdad.
Dr. Fuad T.ibrahim
Collage of science, University of Baghdad/ Baghdad.

Abstract

Pulse laser deposition was used in this research by Nd:YAG laser with (λ=1064 nm average frequency 6 Hz and pulls duration 10 nm) to deposit an adoped ZnO thin films with 0.02 CuO with thickness (100) nm. X-ray diffraction pattern for Zinc oxide films with doping ratio of CuO shows that these films have polycrystalline hexagonal structure, and the X-ray diffraction patterns of porous silicon showed a broadening in the FHWM with increasing etching time. .From atomic force microscope of prepared samples show an average diameter of PS nanostructure. The operation temperature of gas sensor was studied for different temperature and found that the maximum sensitivity is (67.55) at T=350 c^o.

Keywords: metal oxide, gas sensor, Porous silicon.

متحسس غاز الهايدروجين لاوكسيد الخارصين المشوب بالنحاس على قواعد مسامية للجسيمات النانوية

الخلاصة

تم في هذا البحث استخدام طريقة الترسيب بالليزر النبضي بواسطة ليزر Nd:YAG (ذي الطول الموجي λ=1064 nm وبمعدل تكرار 6 Hz وفترة نبضة 10ns) لترسيب أغشية رقيقة لأوكسيد الخارصين المشوبه بالنحاس وبنسبة 0.02% وبسمك حوالي 100 نانومتر للاغشية المحضرة ، بينت حيود الاشعه السينيه لأغشية أوكسيد الخارصين المشوب بنسب مختلفة بالنحاس بان هذه الاغشية تمتلك تركيب سداسي متعدد التبلور.وان حيود الاشعة السينية للسيليكون المسامي تمتلك تعريض بعرض منتصف القمة عند تيار 40 ملي امبير و زمن التنميش10 دقائق. من دراسة سطح الاغشية بواسطة مجهر القوى الذرّيه تبين أن الحجم الحبيبي للسيليكون المسامي ذو التركيب النانوي.تم دراسة حرارة التشغيل للمتحسس الغازي ووجد ان اعلى قيمة للتحسسية (65.55) عند درجة حرارة 350 سيليزي.

الكلمات المفتاحية :اكاسيد المعادن ,متحسس الغازات ,السيليكون المسامي .

INTRODUCTION

Metal oxide semiconductors such as ZnO [1,2], In_2O_3[3], ,TiO_2[4] , Sb_xO_y [5] . have attracted significant attention towards gas sensing due to their simple implementation, low cost, and good reliability for real-time control systems with respect to other gas sensors. The gas sensing properties of metal oxide semiconductors are influenced by many factors such as their operating temperatures,

http://doi.org/10.30684/etj.2015.116477
2412-0758/University of Technology-Iraq, Baghdad, Iraq

morphology and chemical composition of the films [6] . In such gas sensors the change in the electrical conductivity is due to the interaction of the targeted gas molecules (chemi or physisorption) with the surface of the metal oxide grains. Consequently, metal oxide sensors show changes in the resistance under exposure to oxidizing or reducing gases. [7,8] Since the majority of these sensitive layers are *n*-type , *p*-type semiconductors sensitive to gases are highly demanded for gas sensing applications such as sensor arrays for electronic nose.

In 1990, Yamazoe [9,10] reported that, in a gas sensitive material, the reduction of size of grains to nanostructure dimensions can largely enhance gas sensor performance. By engineering and tuning the morphology of grains the sensitivity can also be increased [11]. The electrical properties of such materials change due to grain coalescence, porosity and grain-boundary alteration [12,13].

In addition, the usage of nanostructures increases the surface to volume ratio which generally enhances the sensor response. The increase in the surface of nanostructured materials can also lead to increase in catalytic activity or surface adsorption [12]. Nowadays, nanostructured materials such as semiconducting metal oxide nanoparticles, nanowires and nanorods have been widely used for gas sensing applications. Examples of such materials include: ZnO nanobelt for NO_2, H_2 and hydrocarbon [14], SnO_2 nanobelts for CO and NO_2 [15], In_2O_3 nanowires for NO2 [16],WO_3 nanowires for NO_2 [17], TiO_2 nanotubes for H_2 [18] and many others.
The diffusion of Cu into ZnO can cause the formation of complex centres (Cu_{Zn} , Cu_i). It is possible that Cu atoms can replace either substitution or interstitial Zn atoms in the ZnO lattice creating structural deformations [19,20] . CuO significantly affects the electrical , chemical, structural and optical properties of ZnO , and the study of the electronic state of Cu in ZnO has been the subject of interest for a long time[21].

Experimental

Zinc Oxide powder with doping concentrations for CuO at 0.02 CuO pressing it under 5 Ton to formed a target with 2.5 cm diameter and 0.2 cm thickness. It should be as dense and homogenous as possible to ensure a good quality of the deposit ZnO with doping rate 0.02 CuO thin films were prepared by PLD technique. The pulsed laser deposition experiment is carried out inside a vacuum chamber generally at (10^{-3} Torr) vacuum conditions. The focused Nd:YAG Q-switching laser beam coming through a window is incident on the target surface making an angle of 45° with it. The substrate is placed in front of the target with its surface parallel to that of the target.

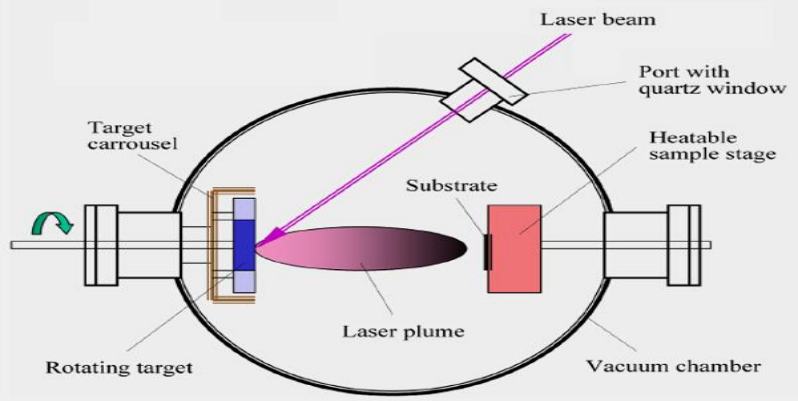

Figure (1) Schematic of PLD system.

Porous silicon prepared by electrochemical Etching were The silicon wafer serves as the anode. The cathode is made of platinum. Si wafer p-type was used as a starting substrate in the photochemical etching. The samples were cut from the wafer and rinsed with acetone and methanol to remove dirt. In order to remove the native oxide layer on the samples, they were etched in diluted HF acid (1:1) with current density 40 mA and etching time 10 min .

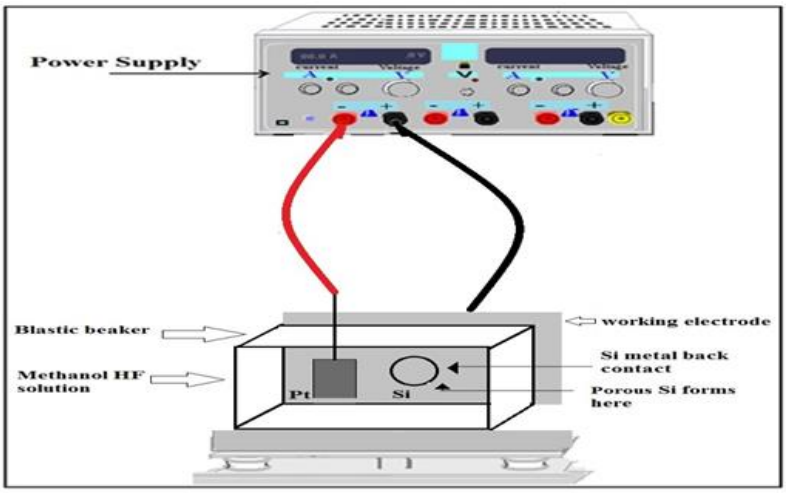

Figure (2) porous silicon experiment set up

In order to study the structural properties, the crystal structure is analyzed with a SHIMADZU 6000 X-ray diffractometer system which records the intensity as a function of Bragg's angle. The source of radiation is Cu (k_α) with wavelength λ=1.5406Å.

The morphological surface analysis is carried out employing an atomic force microscope (AA3000 Scanning Probe Microscope SPM, tip NSC35/AIBS from Angstrom Ad-Vance Inc. The morphological features scanning electron microscopy of the various films are investigated with a JEOL JSM-6360 equipped with a EDAX detector**.**

Result and discussion

X-ray diffraction results

Fig. (3) shows the X-ray diffraction patterns for ZnO with doping ratio 0.02 CuO on a Si (111) substrate . thin films prepared by pulse laser deposition (PLD) technique . We can noticed from x-ray pattern that the peaks (2θ=31.8485, 34.5580, 36.3490) referred to {(100),(002),(101)} direction , respectively . the x-ray diffraction data of thin films coincides with that of known hexagonal structure, Table (3.1) shows the experiment of standard peaks from International Centre for Diffraction (card No. 96-900-8878) . We can observe the peak of Si located at 2 θ=28 which related to Si (111) . The preferred peak for ZnO film doped with 0.02 CuO ratio appear at 2θ =36.3490 for (101) plane this results coincide with M.Rahmani[22].

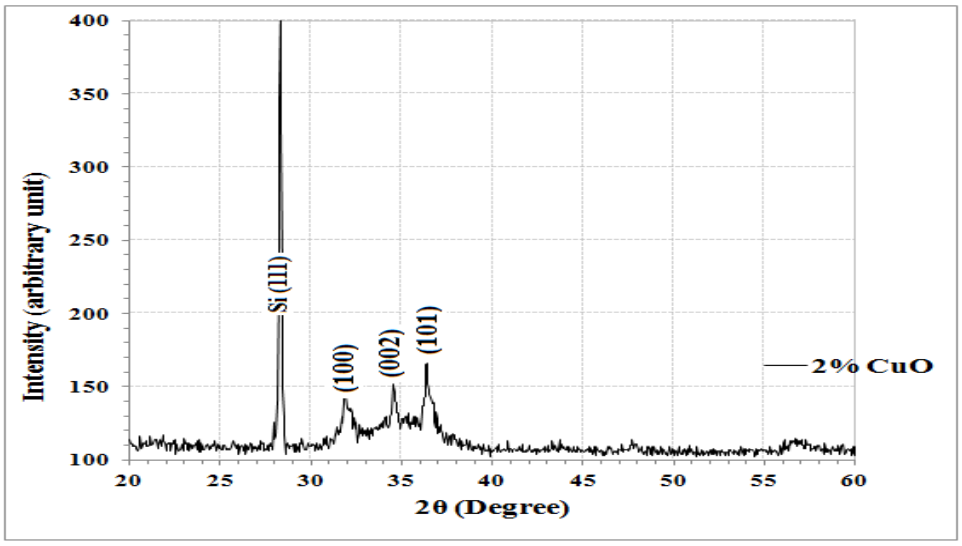

Figure (3) X-ray diffraction patterns of deposited ZnO doped with 0.02 % CuO.

Table (1) Structural parameters: 2θ, d_{hkl}, (hkl), FWHM ad G.S of deposited ZnO films at doping ratio 0.02% CuO.

Cu %	2θ (Deg.)	FWHM (Deg.)	d_{hkl} Exp.(Å)	G.S (nm)	d_{hkl} Std.(Å)	hkl
	31.8944	0.5511	2.804	15.0	2.8137	(100)
2	34.5350	0.2985	2.595	27.9	2.6035	(002)
	36.3720	0.4363	2.468	19.2	2.4754	(101)

Figure (4) shows the porous of p-type Si (111) at current density 40 mA and etching time 10 min . XRD shows the different between Si wafer and porous silicon where. The strong peak of Si fresh appear at 2θ = 28.3721 along the (111) direction is observed confirming the monocrystalline structure of the Si layer which belongs to the (111) reflecting plane of Si cubic structure according to (card NO.96-901-3109). The Table (2) shows the effect of etching time ,this peak becomes broad with varying full-width at half maximum as shown in fig. (2),The additional peak at the lower angle at 2θ=28.3120 may be attributed to a lattice expansion of the porous layers. The presences of this peaks of PS structures shows that the cubic structure of the crystalline silicon is retained even after the pore formation. This observation agrees well with M.Q. Zayer [23]. The thickness of the porous structure is decreasing with increase etching time; the reduction in the crystallite size can be inferred through the increase in broadening of the X-ray diffraction spectra.

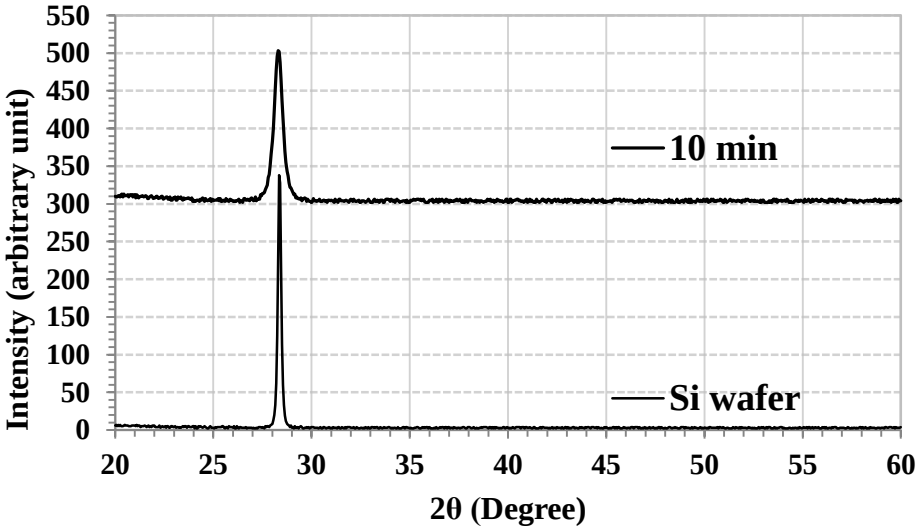

Figure (4) X-ray diffraction patterns of porous silicon at current 40 mA and time 10min

Table (2) Structural parameters: 2θ, d_{hkl}, (hkl), FWHM ad G.S of porous silicon at I=40mA and time (10 min ,50 min).

Sample	2θ (Deg.)	FWHM (Deg.)	d_{hkl} Exp.(Å)	G.S (nm)	d_{hkl} Std.(Å)	hkl
Si wafer	28.3721	0.1860	3.1432	44.0	3.1474	(111)
10 min	28.3120	0.5130	3.1497	16.0	3.1474	(111)

Atomic Force Microscopy (AFM):

The morphological surface analysis is carried out employing an atomic force microscope (AA3000 Scanning Probe Microscope SPM, tip NSC35/AIBS from Angstrom Ad-Vance Inc). Figure (5) shows AFM 3D images of ZnO doped with 0.02 CuO where deposited on glass substrate .AFM parameters (average diameter =83.17, average roughness =6.11 and peak –peak=24.8).

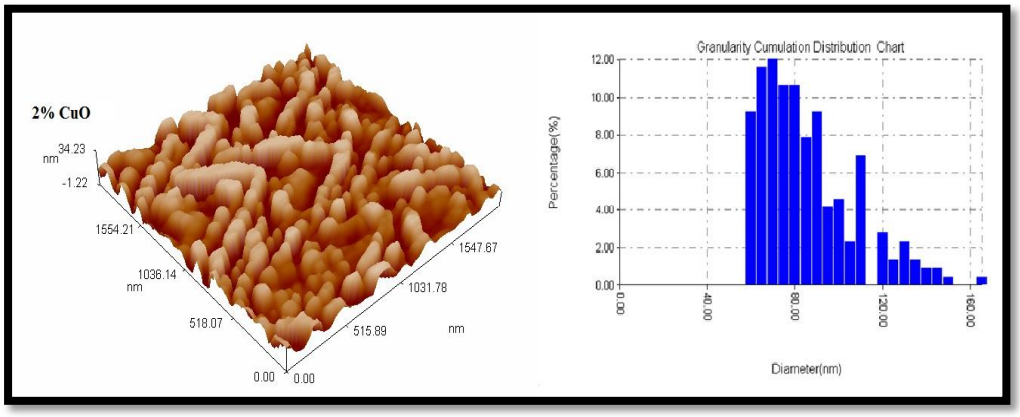

Figure (5) Atomic force microscopy pictures for doped ZnO with 0.02 CuO deposited on glass

Figure (6) shows AFM images of porous silicon at current density 40 mA and etching time 10 min . AFM parameters, average diameter =29.29, average roughness =0.559 and average peak –peak =3.47.

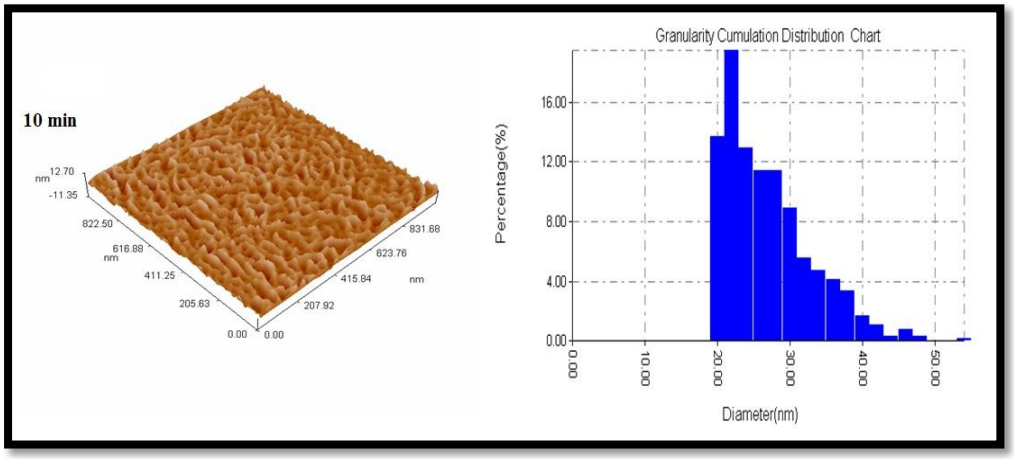

Figure (6) Atomic force microscopy picture for Porous Si wafer with constant current I=40 mA and etching time 10 min.

Scanning electron microscopy (SEM)

Figure (7) show scanning electron microscopy of ZnO doped with 0.02 CuO on silicon (111) substrate by pulse laser deposition technique.

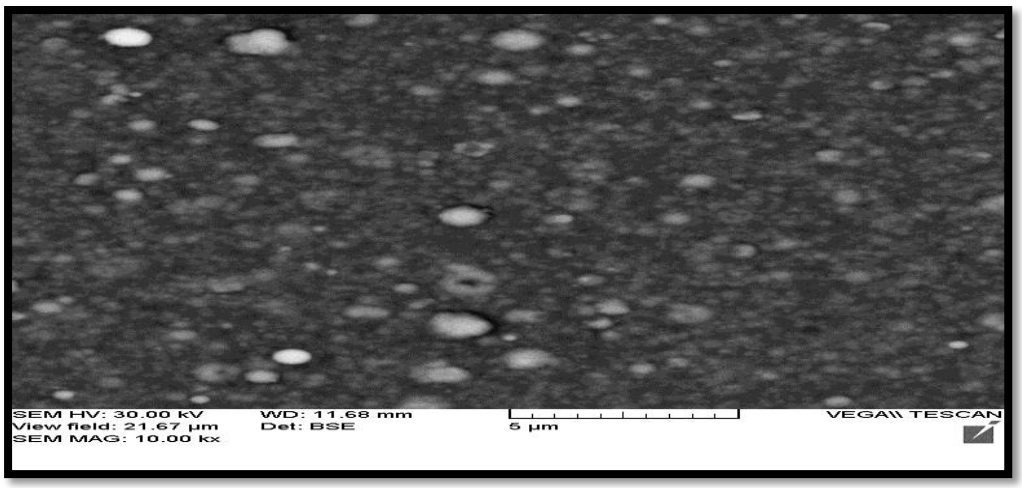

Figure(7) SEM images for ZnO doped with 0.02 CuO thin films

Gas sensor

Figure (8) shows the sensitivity as a function of operation temperature in the range (Rt-350 $^{\circ}$C) for ZnO doping with 0.02 CuO which are deposited on porous Si wafer (111) for 10min etching time. It can be seen in Figure (8) that the sensitivity of the films increases with the increasing in the operating temperature, reaching a maximum value corresponding to an optimum operating temperature which is 350°C for the sample. The high temperature operation of the sensor make the life time of the sensor become shorter and increasing resistance thus required more electricity for operation . It is believed that the oxygen could be removed or lost from the bulk of the metal

oxide materials at high temperatures. This suggests that the response of the sensor may decrease at higher temperatures since there will be more oxygen vacancies which led to less occurrence of hydrogen oxygen reaction.

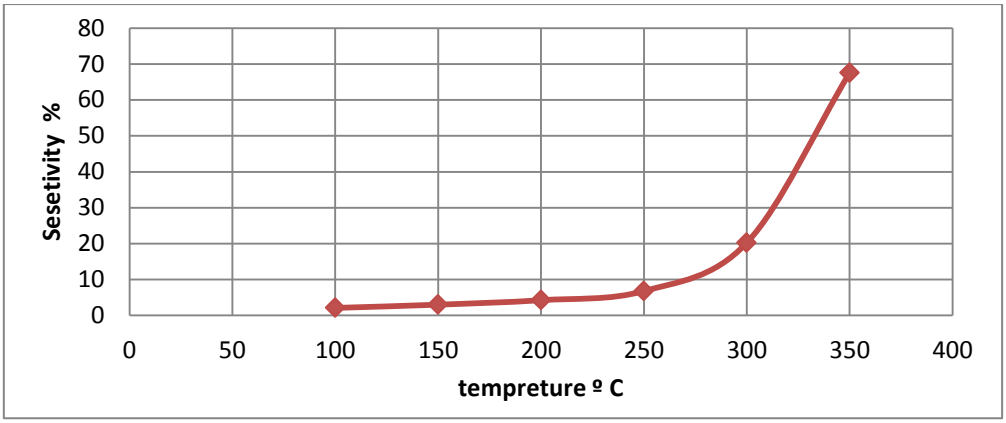

Figure (8) The variation of sensitivity with the operating temperature for 10 Etching time on porous silicon.

Figure (9) exhibits the transient response as a function of hydrogen gas concentration for the ZnO doping with 0.02 CuO which are deposited on porous Si wafer (111) sensing element at 300^{o} C. The sensitivity of the gas sensor increases as the hydrogen gas concentration is increased from 5% , 10%, 15% and 20% , and it drops relatively rapidly when the testing gas is removed , indicating that the gas sensor has a good response for different hydrogen concentrations. Besides, it takes almost the same time for the sensor to reach the maximum sensitivity for different hydrogen concentrations. This result is consistent with the conclusion for the dominance of operation temperature for the response time [64]. As it is apparent from the figures, the sensor sensitivity to hydrogen gas was increases linearly with test gas mixing ratio up to 15% at which the lowest response and recovery times of 20.7s and 2.7s. The maximum sensitivity record (67.55%) for the sample prepared at 10min etching time. The gas sensor system is designed and testing in thin-film laboratory – department of physics-college of science- university of Baghdad.

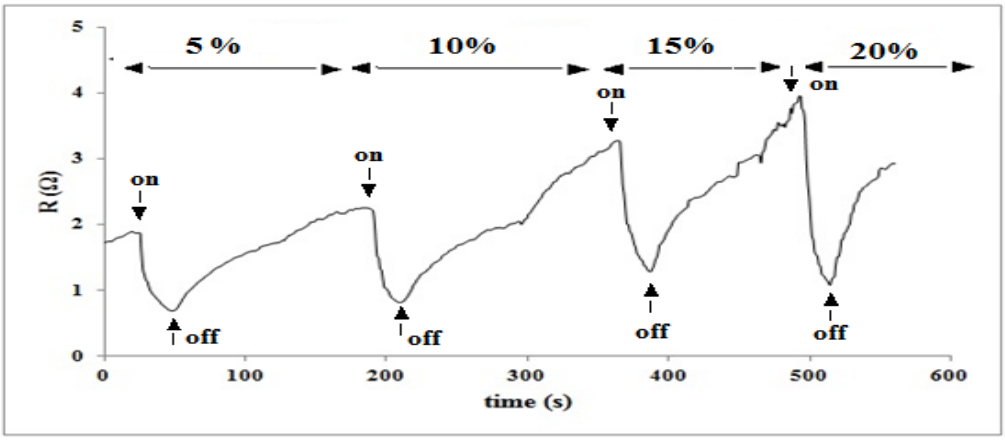

Figure (7) The variation resistance with time for different hydrogen gas concentration for the porous silicon gas sensor.

Conclusions

1. A polycrystalline structure for CuO doped ZnO prepared successfully by PLD.
2. A topography of porous Si shows an decrease in average diameter with increase etching time.
3. PL emission spectrum has abroad blue range with increasing porosity time.
4. Sensitivity of Hydrogen gas sensor increasing with increase operation temperature

Reference

[1] A. Z. Sadek, W. Wlodarski, Y. X. Li, W. Yu, X. Li, X. Yu, and K. Kalantar-Zadeh, Thin Solid Films 515/24, 8705 (2007).
[2] A. Z. Sadek, S. Choopun, W. Wlodarski, S. J. Ippolito, and K. Kalantar-Zadeh, IEEE Sens. J. 7/5–6, 919 (2007).
[3] S. J. Ippolito, S. Kandasamy, K. Kalantar-Zadeh, W. Wlodarski, K. Galatsis, G. Kiriakidis, N. Katsarakis, and M. Suchea, Sens. Actuators, B: Chemical 111–112, 207 (2005).
[4] J. Tan, W. Wlodarski, and K. Kalantar-Zadeh, Thin Solid Films 515/24, 8738 (2007).
[5] R. Arsat, S. J. Tan, W. Modarski, and K. Kalantar-Zadeh, Sensor Lett. 4, 419 (2006).
[6] Y. Shen, T. Yamazaki, Z. Liu, D. Meng, T. Kikuta, and N. Nakatani, Thin Solid Films 517/6, 2069 (2009).
[7] L. A. Obvintseva, Russian J. General Chemistry 78/12, 2545 (2008).
[8] H. Gong, J. Q. Hu, J. H. Wang, C. H. Ong, and F. R. Zhu, Sens. Actuators, B: Chemical 115/1, 247 (2006).
[9] N. Yamazoe, "New approaches for improving semiconductors gas sensors " in Proc. 3rd International Meeting on Chemical Sensors, Cleveland, OH, U.S.A., 1990, pp. 3-8.
[10] N. Yamazoe, "New approaches for improving semiconductor gas sensors," Sensors and Actuators B: Chemical, vol. 5, pp. 7-19, 1991.
[11] N. Barsan, M. Schweizer-Berberich, and W. Gopel, Fresenius Journal of Analytical Chemistry, vol. 365, pp. 287-304, 1999.
[12] E. Comini, "Metal oxide nano-crystals for gas sensing," Analytica Chimica Acta, vol. 568, pp. 28-40, 2006.
[13] K. Kalantar-zadeh and F. Benjamin, Nanotechnology-Enabled Sensors. Springer, 2008.
[14] A. Z. Sadek, S. Choopun, W. Wlodarski, S. J. Ippolito, and K. Kalantar-zadeh, "Characterization of ZnO nanobelt-based gas sensor for H2, NO2, and hydrocarbon sensing," IEEE Sensors Journal, vol. 7, pp. 919-924, 2007.
[15] E. Comini, G. Faglia, G. Sberveglieri, Z. Pan, and Z. L. Wang, "Stable and highly sensitive gas sensors based on semiconductiong oxide nanobelts," Appl. Phys. Lett, vol. 81, pp. 1869- 1871, 2002.
[16] D. Zhang, Z. Liu, C. Li, T. Tang, X. Liu, S. Han, B. Lei, and C. Zhou, "Detection of NO_2 down to ppb levels using individual and multiple In2O3 nanowire devices," NanoLetters, vol. 4, no. 10, pp. 1919-1924, 2004.
[17] K. M. Sawicka, A. K. Prasad, and P. I. Gouma, "Metal oxide nanowires for use in chemical sensing applications," Sensor Letter, vol. 3, no. 1, pp. 1-5, 2005.

[18] H. Y. Dang, J. Wang, and S. S. Fan, "The synthesis of metal oxide nanowires by directly heating metal samples in appropriate oxygen atmospheres," Nanotechnology, vol. 14, pp. 738-741, 2003.
19. M. Oztas and M. Bedir, Thin Solid Films 516/8, 1703 (2008).
[20] J. B. Kim, D. Byun, S. Y. Ie, D. H. Park, W. K. Choi, C. Ji-Won, and A. Basavaraj, Semicond. Sci. Technol. 9, 095004 (2008).
[21] G. H. Kim, D. L. Kim, B. D. Ahn, S. Y. Lee, and H. J. Kim, Microelectron. J. , (2009)**,**272**.**
[22] M. B. Rahmani,S. H. Keshmiri, M. Shafiei, K. Latham, W. Wlodarski,J. du Plessis, and K. Kalantar-Zadeh, School of Applied Sciences, RMIT University,(2009)1-8.
[23] M.Q. Zayer, **,** M.Sc. Thesis University of Technology Applied Sciences Department Laser Division (2010).
[24] y.y.abdul M.Ismail,M.N .Mdyusuf.W.N.W.shamsuri"the effect of thickness on ZnO thin film CO gas sensor" , university of technology malysia,(2006) .p 89-94.